Crystal Chemistry and Structure of the Orthorhombic (Fe,Mn)(Ta,Nb)$_2$O$_6$ Family of Compounds

C.A. dos Santos*, L.I. Zawislak, E.J. Kinast, V. Antonietti, and J.B.M. da Cunha

Instituto de Física, Universidade Federal do Rio Grande do Sul,

Campus do Vale, C.P. 15051, 91501-970 Porto Alegre, RS, Brazil

Received on 19 July, 2001

In this paper we review the crystal chemistry and structure data from the literature and our results reported in the last decade for natural and synthetic samples of the tantalite-columbite series. Order-disorder transitions and oxidation reactions on the ixiolite-columbite-wodginite system are reported for one Brazilian sample. It is shown that reports on these subjects are sometimes dubious and incomplete. In addition to the reaction atmosphere (air or vacuum), order-disorder and oxidation are strongly dependent on the physical state of the samples (powdered or crystal). Structure and chemical composition have been investigated in our laboratory using X-ray diffraction (XRD), electron probe microanalysis (EPMA) and Mössbauer spectroscopy (MS).

I Introduction

The (Fe,Mn)(Ta,Nb)$_2$O$_6$ family of compounds encompasses two different solid solutions. One, orthorhombic, is named tantalite-columbite and the other one, tetragonal, is named tapiolite-mossite [1-9]. Besides their economical importance (they are the major source of tantalum) these materials present interesting physical properties which have motivated investigations reported in the last two decades [10-18].

For long time and even in some modern reports, these solid solutions were considered continua. In such scenery both solid solutions would have $FeTa_2O_6$, $FeNb_2O_6$, $MnTa_2O_6$ and $MnNb_2O_6$ as end-members. These compounds were proposed with different denominations for each series.[19] The orthorhombic series would be comprised of ferrotantalite ($FeTa_2O_6$), ferrocolumbite ($FeNb_2O_6$), manganotantalite ($MnTa_2O_6$) and manganocolumbite ($MnNb_2O_6$). On the other hand the tetragonal series would include ferrotapiolite ($FeTa_2O_6$), ferromossite ($FeNb_2O_6$), manganotapiolite ($MnTa_2O_6$) and manganomossite ($MnNb_2O_6$). However, it is now well established that each series has limited solubility [19-26]. For example, long time ago Hutchinson[20] has questioned the existence of the mineral mossite (tetragonal (Fe,Mn)Nb_2O_6) and since then none such natural sample has been reported.[26] In spite of the fact that Aruga *et al.*[27] have described a synthetic $FeNb_2O_6$ sample with a disordered ferromossite structure, today the tetragonal series is simply named tapiolite, whose Mn and Nb solubility are limited to less than 50 at.%. Although the orthorhombic series continue to be named tantalite-columbite,[26] single-phase species of tantalite (orthorhombic $FeTa_2O_6$) have not yet been reported as natural occurrence or as synthetic one.

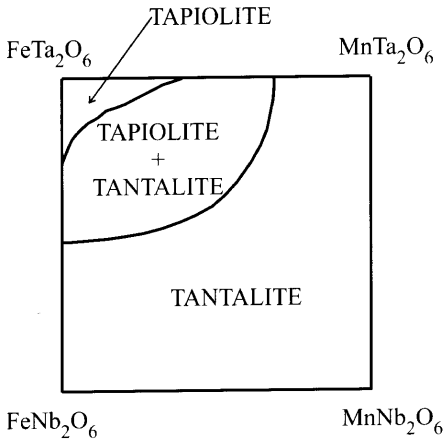

Figure 1. Sketch of the compositional field for the AB_2O_6 system.

A schematic compositional field for natural samples, based on a recent paper by Wise and Cerny,[26] is presented in Fig. 1. Clark and Fejer[24] suggested that

*Corresponding author; e-mail: cas@if.ufrgs.br

the solubility limit in this series depends strongly on the crystallization history for both synthetic and natural samples. This is evident from results reported for synthetic samples. Moreau and Tramasure[5] reported a solubility limit of 15 at.% Nb for the tapiolite solid solution, while dos Santos and Oliveira[12] extended this limit to 45 at. % Nb.

In addition to this question about the solubility limit, the orthorhombic series has been the subject of several investigations (for a review, see[8, 22, 23]) on order-disorder phenomena connecting tantalite-columbite and the minerals wodginite[1] and ixiolite.[2] From the structural point of view it is sure that an order-disorder transition can transform ixiolite into tantalite-columbite or into wodginite. However, as will be discussed below, it is not yet known if the alternative transformations are governed by geochemical, or simply by crystallochemical factors.

Interest in these materials has recently increased motivated by its magnetic properties. In tetragonal $FeTa_2O_6$ the sublattice formed by the iron atoms has the same symmetry as the Ni sublattice in the body-centered tetragonal K_2NiF_4 compound, the well-known two-dimensional Heisenberg antiferromagnet. As expected, the magnetic behavior of $FeTa_2O_6$ is analogous to that of the K_2NiF_4. For example, in both compounds the susceptibility has a broad maximum and falls off slowly in the paramagnetic region, a characteristic associated with planar magnets.[10, 13, 28, 29] Another interesting point is that while $FeTa_2O_6$ presents uniaxial anisotropy on the basal plane, the isomorphous compound $CoTa_2O_6$ presents a very complex two-cone axis helical spin structure[30] with components on the basal plane as well as on the c-direction. Such features suggest that $Fe_xCo_{1-x}Ta_2O_6$ could present competing anisotropies.

The systems with competing anisotropies lead to a tetracritical phase transition, [31-33] whose experimental confirmation has been reported for several materials, between them $K_2Co_xFe_{1-x}F_4$.[34, 35] Keeping in mind the similarities between K_2NiF_4 and $FeTa_2O_6$ compounds, it is expected $Fe_xCo_{1-x}Ta_2O_6$ to present some kind of competing anisotropies behavior. Indeed, these mixed oxides have been recently prepared,[14, 15] but the competing anisotropies behavior was not observed in the preliminary magnetic measurements performed.

In this paper we review the crystal chemistry and structure data from the literature and our results reported in the last decade for natural and synthetic samples of the tantalite-columbite series. Structure and chemical composition have been investigated in our laboratory using X-ray diffraction (XRD), electron probe microanalysis (EPMA) and Mössbauer spectroscopy (MS) measurements.

II Crystal chemistry and structure

There is no doubt that the compounds $(Fe,Mn)(Ta,Nb)_2O_6$, with different Fe/Mn and Ta/Nb ratios, are the more representative of the AB_2O_6 series. However, these materials can have minor substitutions of Mg, Sn, W and Ti[8, 19, 22] and can also be synthesized with A=Ni,[18, 36] Co,[14, 15, 37, 38] Cu, [17,39-41] Zn[41] and B=Sb.[30]

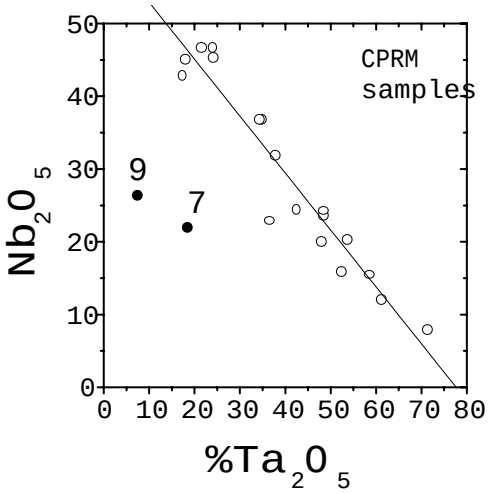

Figure 2. Nb_2O_5 vs Ta_2O_5 concentration for Brazilian tantalite-columbite samples.

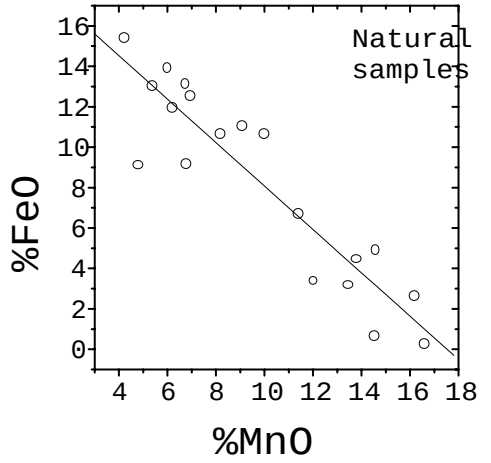

Figure 3. FeO vs MnO concentration for natural samples, taken from [11,22,41-44].

Fig. 2 and Fig. 3 illustrate the correlation between Nb and Ta contents and between Fe and Mn for, respectively, twenty powder samples supplied by the Brazilian company CPRM (Company for Research of Mineral Resources) and for natural samples reported by other

Table 1: Mean chemical composition (wt.%) based on 6 oxygens, from EPMA measurements.

Sample	FeO	MnO	Ta_2O_5	Nb_2O_5	TiO_2	WO_3	TOTAL
$Fe_{0.1}Mn_{0.9}Ta_{1.8}Nb_{0.2}O_6$	1.67	12.87	78.69	5.61	0.21	—	99.05
$Fe_{0.1}Mn_{0.8}Ta_{1.7}Nb_{0.3}O_6$	1.54	12.77	77.62	6.38	0.39	0.29	98.99
$Fe_{0.6}Mn_{0.4}Ta_{1.3}Nb_{0.7}O_6$	8.87	6.85	59.12	21.95	1.59	—	98.38

authors.[11,22,41-44] The samples labeled 7 and 9 in Fig. 2, clearly out of the linear fitting, are Sn- and Ti-rich samples (7: 1.9 %SnO_2 / 20 %TiO_2; 9: 7.9 %SnO_2 / 23.3 %TiO_2). Therefore, these samples present low Nb+Ta concentration ($\simeq$ 64 and 42 wt.%, respectively) as compared to the mean concentration of the CPRM collection ($\simeq$ 73 wt.%).

Yet, the strong correlation between Fe and Mn contents and between Ta and Nb ones can be nicely appreciated by scanning crystal samples with EPMA.

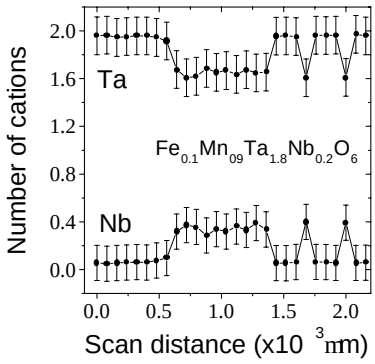

Figure 4. Nb and Ta microprobe scans for the Brazilian $Fe_{0.12}Mn_{0.83}Ti_{0.01}Ta_{1.78}Nb_{0.24}O_6$ sample.

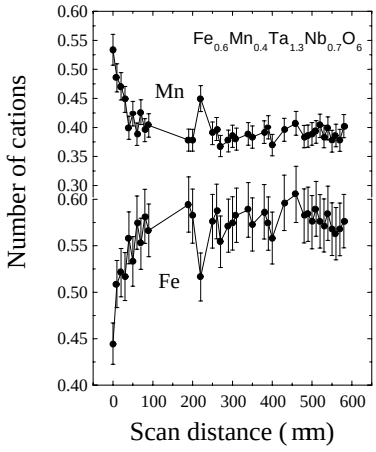

Figure 5. Mn and Fe microprobe scans for the Brazilian $Fe_{0.57}Mn_{0.38}Ti_{0.10}Ta_{1.26}Nb_{0.68}O_6$ sample.

Fig. 4 shows the amount of Ta and Nb, in atoms per formula unit (apfu), measured along a line 2 mm long in the Brazilian $Fe_{0.1}Mn_{0.9}Ta_{1.8}Nb_{0.2}O_6$ sample (see Table 1 for the complete chemical composition). Ta-rich zones correspond to Nb-poor ones and vice versa, with Ta+Nb$\simeq$2.0 apfu. A similar result for Fe and Mn is illustrated in Fig. 5 for the Brazilian $Fe_{0.6}Mn_{0.4}Ta_{1.3}Nb_{0.7}O_6$ sample. In this case Fe+Mn$\simeq$1.0 apfu.

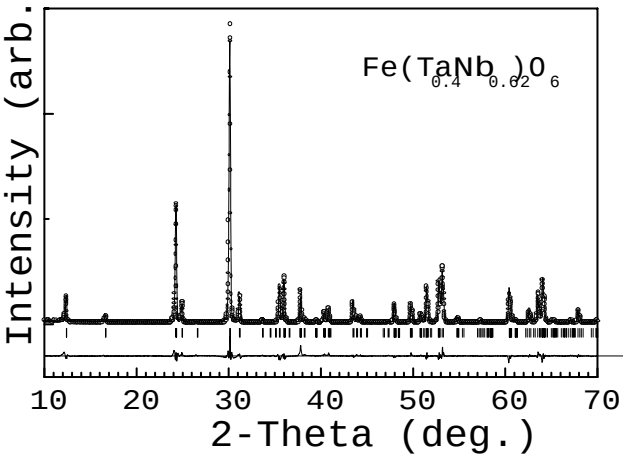

Figure 6. Representative part of the room-temperature X-ray powder diffraction pattern for the synthetic $Fe(Ta_{0.4}Nb_{0.6})_2O_6$ sample. Open circles represent observed data. The solid line represents the calculated pattern obtained with the Rietveld refinement. The lower trace is a plot of the residual spectrum, observed minus calculated intensities.

A typical XRD pattern is shown in Fig. 6 for a synthetic ferrocolumbite sample, with composition $Fe(Ta_{0.4}Nb_{0.6})_2O_6$. It was prepared by mixing appropriate amounts of powdered Fe, Fe_2O_3, Ta_2O_5 and Nb_2O_5. Pellets of the mixture were heated under a nitrogen flow at 1320 K. After 24 h it was cooled at 15 K/h. New pellets were again submitted to the same heat treatment for 24 h, followed by the same slow cooling. Hereafter this synthetic sample will be called $Fe(Nb,Ta)_2O_6$. The pattern was indexed[45, 46] to the space group Pbcn with crystallographic parameters as displayed in Table 2. Projections of the refined struc-

Table 2: Atomic parameters for $Mn_{0.88}Fe_{0.09}Ta_{1.72}Nb_{0.28}O_6$ and $Fe(Ta_{0.4}Nb_{0.6})_2O_6$. Space group Pbcn. $R_B = 100 \sum |I_{obs} - I_{calc}| / \sum I_{obs}$.

Sample/Atom	x	y	z	R_B
(Mn,Fe)(Ta,Nb)$_2$O$_6$	a=14.3196(9) (Å)	b=5.7413(4) (Å)	c=5.0624(3) (Å)	5.76
(Fe,Mn)	0	0.327(2)	0.25	
(Nb,Ta)	0.1618(2)	0.1812(4)	0.743(1)	
O1	0.099(1)	0.102(3)	0.067(5)	
O2	0.419(1)	0.115(3)	0.072(5)	
O3	0.769(2)	0.126(3)	0.099(4)	
Fe(Nb,Ta)$_2$O$_6$	a=14.2737(2) (Å)	b=5.73543(1) (Å)	c=5.0554(1) (Å)	5.55
Fe	0	0.335(9)	0.25	
(Nb,Ta)	0.1618(8)	0.179(2)	0.744(4)	
O1	0.096(4)	0.11(0)	0.06(8)	
O2	0.418(8)	0.11(8)	0.07(8)	
O3	0.765(8)	0.11(6)	0.08(6)	

Table 3: Cell unit parameters for natural tantalite-columbite samples.

Sample	a(Å)	b(Å)	c(Å)	%order	Ref.
$(Fe_{0.01}Mn_{0.97})(Ta_{0.64}Nb_{0.36})_2O_6$	14.413	5.760	5.084	101	22
$(Fe_{0.09}Mn_{0.88})(Ta_{0.86}Nb_{0.14})_2O_6$	14.320	5.741	5.062	101	45
$(Fe_{0.19}Mn_{0.79})(Ta_{0.61}Nb_{0.39})_2O_6$	14.300	5.741	5.124	38	42
$(Fe_{0.23}Mn_{0.72})(Ta_{0.61}Nb_{0.39})_2O_6$	14.288	5.753	5.167	-5	44
$(Fe_{0.38}Mn_{0.62})(Ta_{0.09}Nb_{0.91})_2O_6$	14.311	5.742	5.101	62	42
$(Fe_{0.46}Mn_{0.53})(Ta_{0.28}Nb_{0.72})_2O_6$	14.295	5.729	5.113	47	42
$(Fe_{0.54}Mn_{0.42})(Ta_{0.15}Nb_{0.85})_2O_6$	14.400	5.775	5.092	90	43
$(Fe_{0.63}Mn_{0.41})(Ta_{0.20}Nb_{0.78})_2O_6$	14.258	5.731	5.086	65	42
$(Fe_{0.64}Mn_{0.34})(Ta_{0.24}Nb_{0.73})_2O_6$	14.189	5.727	5.120	18	11
$(Fe_{0.68}Mn_{0.28})(Ta_{0.25}Nb_{0.75})_2O_6$	14.221	5.727	5.102	42	11

ture along the a and c directions are shown in Figs. 7(a) and 7(b), respectively. Such orthorhombic AB_2O_6 structure can be derived from a hexagonal closed packing of oxygen ions. Within the b-c plane half of the oxygen octahedra are occupied by metal ions (A or B) forming zigzag chains of edge-sharing MO_6 octahedra running along the c-axis. Within the a-b plane the layers are stacked up in an order A-B-B-A-B-B-A. The three independent oxygen atoms are all three-coordinated: O1 bridging one A and two B atoms, O2 bridging two A atoms and one B atom and O3 bridging three B atoms.

As expected for solid solution, the unit cell dimensions would obey the Vegard's law. This means, the unit cell parameters would be a linear function of the cation ionic radii on the A and B sites. As an illustration we present in Table 3 the cell unit parameters for some natural tantalite-columbite samples with different Fe/Mn and Ta/Nb ratios. The b and c parameters display scattered data as a function of both A and B sites. The a parameter data are very scattered when plotted against the B site content. Only cation substitution in the A site obeys reasonably the Vegard's law. There are several factors contributing for such a behavior. The only investigated in some extent will be discussed in section III and concerns to order-disorder transition. Other intervening factors are minor substitutions of Ti, Sn and W, as well as the uncontrollable crystallization history.

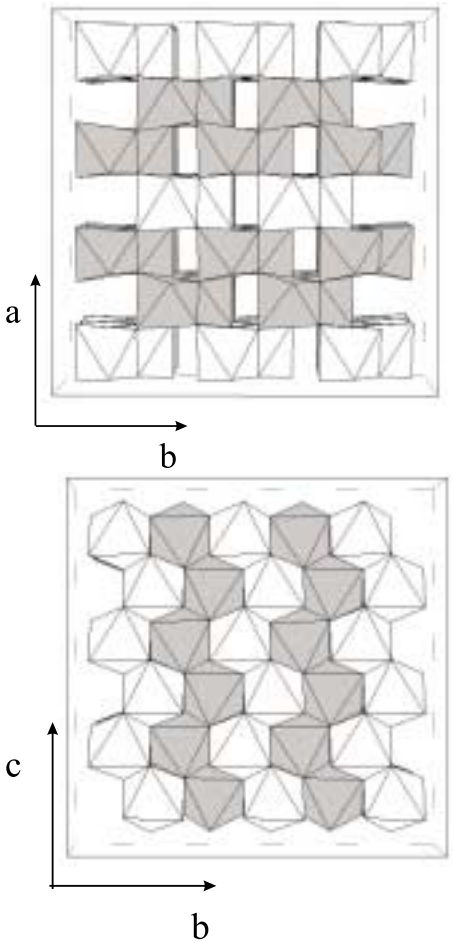

Figure 7. Coordination polyhedron chains stacked along (a) a-axis and (b) c-axis of the columbite structure.

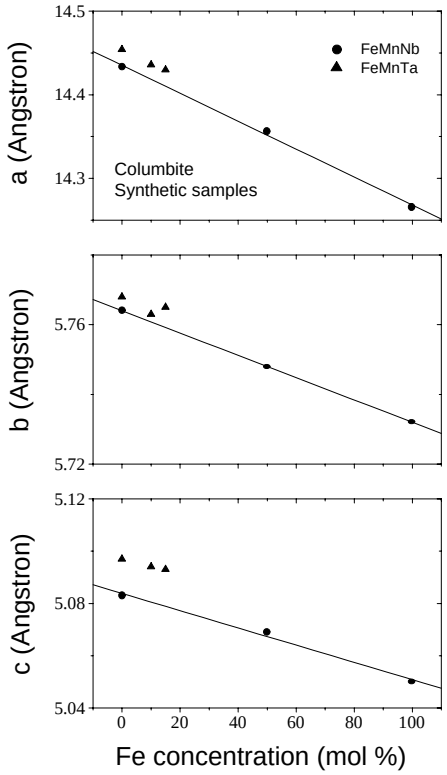

Figure 8. Cell unit parameters as a function of Fe concentration for synthetic columbite samples. Data from Table 4.

For synthetic samples prepared with the same procedure, irrespective of the special kind of route, the Vegard's law is fairly illustrated in Table 4 and Fig. 8 for the $Fe_xMn_{1-x}Nb_2O_6$ and $Fe_xMn_{1-x}Ta_2O_6$ series.[6, 47] These results suggest that Nb $\rightarrow$ Ta substitution has minor effect on the cell dimensions, while Fe$\rightarrow$ Mn substitution strongly affects these crystallographic parameters. As shown in Fig. 9 for ANb_2O_6 synthetic samples, with A=Mn, [47] Fe, [47] Co, [38] and Ni,[36] the cell unit dimensions vary linearly with the ionic radii (Mn^{2+}=0.80, Fe^{2+}=0.76, Co^{2+}=0.74, Ni^{2+}=0.72) in agreement with the Vegard's law. However, all the $CuNb_2O_6$ samples reported [17,39-41] are clearly out of the Vegard's law fitting. Such a behavior could be explained by a strong Jahn-Teller effect.

Another way to summarize the crystallographical data from the columbite-tantalite series is by plotting the c against the a parameter. Indeed, the a-c plot[42, 43, 48, 49] has been considered the most appropriate procedure because it enables us to connect crystallographical data to cation ordering features, as discussed in the following.

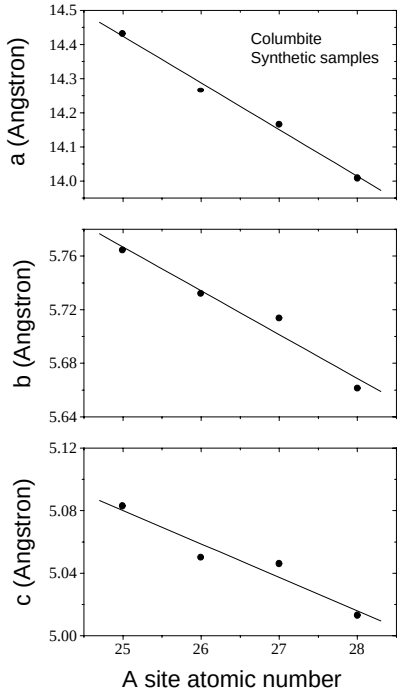

Figure 9. Cell unit parameters as a function of the A site atomic number. Data from Table 4.

Table 4: Cell unit parameters for synthetic tantalite-columbite samples.

Sample	a(Å)	b(Å)	c(Å)	%order	Ref.
$MnNb_2O_6$	14.433	5.764	5.083	97	47
$MnTa_2O_6$	14.454	5.768	5.097	97	6
$(Fe_{0.1}Mn_{0.9})Ta_2O_6$	14.436	5.763	5.094	96	6
$(Fe_{0.15}Mn_{0.85})Ta_2O_6$	14.430	5.765	5.093	96	6
$(Fe_{0.5}Mn_{0.5})Nb_2O_6$	14.356	5.748	5.069	102	47
$Fe(Ta_{0.4}Nb_{0.6})_2O_6$	14.274	5.735	5.055	97	45
$FeNb_2O_6$	14.266	5.732	5.050	100	47
$FeNb_2O_6$	14.263	5.732	5.038	111	57
$FeNb_2O_6$	14.070	5.616	4.978	125	16
$FeNb_2O_6$	14.237	5.732	5.043	101	18
$CoNb_2O_6$	14.167	5.714	5.046	82	38
$NiNb_2O_6$	14.010	5.661	5.013	79	57
$NiNb_2O_6$	14.014	5.682	5.024	70	18
$CuNb_2O_6$	14.103	5.609	5.122	-3	39
$CuNb_2O_6$	14.104	5.607	5.124	-5	40
$CuNb_2O_6$	14.019	5.623	5.107	-7	17
$CuNb_2O_6$	14.097	5.613	5.123	-5	41
$(Cu_{0.36}Zn_{0.64})Nb_2O_6$	14.187	5.730	5.031	101	41

III Cation ordering on the ixiolite-columbite-wodginite system

Ixiolite, with general formula MO_2 (M=Mn, Sn, Fe, Ta, Nb, Ti), is a columbite substructure.[2] Due to this relationship, disordered columbite was formerly called pseudo-ixiolite. Today the inappropriateness of this denomination is well established,[22] but immediately after its suggestion a vivid debate was established on the literature to distinguish true-ixiolite from pseudo-ixiolite. Nickel *et al.*[2] suggested that ixiolite reveal olovotantalite XRD pattern upon heating, while Grice *et al.*[22] proposed that the obtained compound is wodginite. In fact, olovotantalite is identified with orthorhombic wodginite.[2, 5, 50] On the other hand, disordered columbite yields an ordered columbite pattern[2, 8, 22] upon heating.

Wodginite, with the general formula ABC_2O_8 (A = Mn, Fe^{2+}; B = Sn, Ti, Fe^{3+}, Ta; C = Ta, Nb), crystallizes in the monoclinic space group C2/c.[23, 51] Idealized sections of these structures, projected along the a-axis, are outlined in Fig. 10. The A and B octahedra in Fig. 10 refer to the wodginite structure. For columbite both octahedra correspond to the A site, occupied by Fe and Mn cations, while the C sites for wodginite correspond to the B sites for columbite, occupied by Ta and Nb cations. In the wodginite structure, one layer of C cations follows each layer of A+B cations. In the columbite structure, layers of A cations at x=0 and 1/2, are separated by two layers of B cations at x=1/6 and 2/6. Previous structure investigations[8, 23] have shown that columbite and wodginite can be considered as different superstructures of the α-PbO_2-like structure of ixiolite.

Order-disorder phenomena connecting these minerals have been extensively investigated.[8,11,22,23,25,47, 52-54] In the context of the present discussion, an ordered columbite means all Fe and Mn occupying the A site, while all Ta and Nb occupy the B site. It does not means order between Mn and Fe on A sites, nor between Ta and Nb on B sites; a similar approach is applied to the wodginite structure. Cation ordering in MO_2 structure is possible if the unit cell size is increased.[48] To satisfy symmetry restrictions on this process, two alternatives are possible (see Fig. 11). In the first one the MO_2 cell is tripled, given the AB_2O_6 structure. In the other alternative the cell is quadrupled, given the ABC_2O_8 structure.

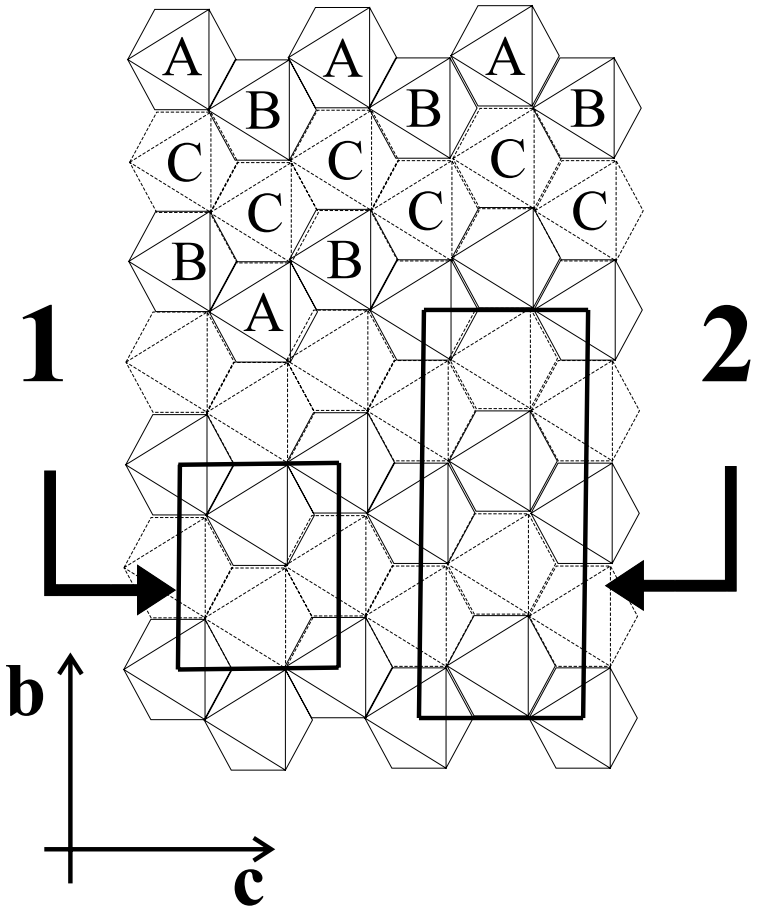

Figure 10. Idealized section of the α-PbO_2 structure projected along the a-axis. A, B and C refer to the cations on the general formula, ABC_2O_8, for wodginite. Occupied octaedra in the upper level are shown in full lines; those occupied in the next level down are shown in broken lines. The columbite and ixiolite cells are represented by the rectangle (1), while rectangle (2) represents the wodginite cell. Ixiolite cell is one double layer deep, wodginite is two double layers deep, and columbite is three double layers deep.

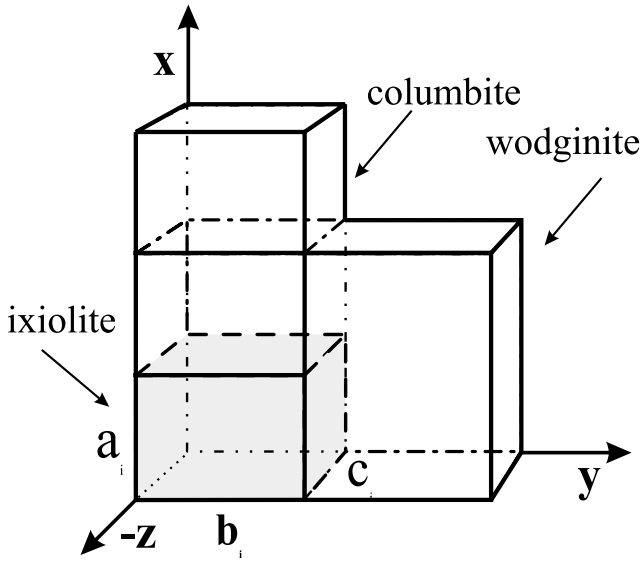

Figure 11. Orientation and volume relationships among ixiolite, columbite and wodginite cell units.

Therefore, fully disordered AB_2O_6 and ABC_2O_8 compounds can be misidentified as MO_2 compounds. This fact has produced considerable experimental mistakes and misconceptions, as reported during the last three decades. For instance, heating experiments have been used to distinguish these materials, with the generally accepted assumption that heating the mineral ixiolite reveals a wodginite XRD pattern, whereas heating the disordered columbite yields an ordered columbite pattern characterized by its superstructure reflections.[2] However, calculation of a theoretical powder diffraction pattern of fully ordered manganocolumbite, $MnNb_2O_6$, yields only low intensities for the superstructure reflections, namely I_{200}/I_{311}=0.096 and I_{110}/I_{311}=0.030.[11] Thus, it is difficult to distinguish between MO_2 and partially ordered AB_2O_6 by means of their XRD patterns, even when done by complex and time-consuming procedures based on the Rietveld refinement.

Table 5: Cell unit parameters for as-collected ixiolite samples. Taken from Cerny *et al.*[50]

	K-1	MSX	NST/A	NST/B	KVV	BRD/C	AMB
a (Å)	14.259	14.205	14.352	14.330	14.127	14.238	14.184
b (Å)	5.730	5.728	5.724	5.740	5.712	5.728	5.709
c (Å)	5.095	5.120	5.088	5.095	5.107	5.088	5.113
$\%order$	56.527	21.145	83.513	72.098	16. 281	58.513	23.131

Table 6: Cell unit parameters for heated (1000 °C, 16 hours in air) ixiolite samples. Taken from Cerny *et al.*[50]

	K-1	MSX	NST/A	NST/B	KVV	BRD/C	AMB
a (Å)	14.284	14.261	14.378	14.370	14.233	14.269	14.255
b (Å)	5.733	5.731	5.742	5.748	5.720	5.722	5.713
c (Å)	5.072	5.072	5.081	5.074	5.056	5.060	5.065
$\%order$	83.67	78.62	95.80	100.64	87.548	91.676	83.898

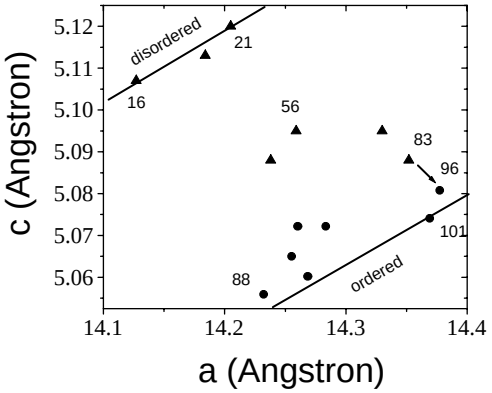

Figure 12. *c*-*a* plot for natural columbite samples. The number near the symbols are the respective EOP. Triangles represent the ordered ones. Data from Tables 5 and 6.

Other criteria have been tentatively established to estimate the degree of cation order. In his PhD thesis, Ercit has derived the following equation for the orthorhombic $(Fe,Mn)(Ta,Nb)_2O_6$ system:[54]

$$\text{percent order} = 1727 - 941.6(c - 0.2329a), \quad (1)$$

where a and c are the lattice parameters. The Ercit's order parameter (EOP) has been obtained from the so-called *a*-*c* plot, mainly for samples submitted to heating experiments. As an illustration let us examine the data summarized in Tables 5 and 6, taken from Cerny *et al.*[50] The as-collected samples (Table 5) were indexed to the ixiolite structure with average cell unit parameter a≃4.747 *Å*. However, for comparison purposes with the ordered columbite phase this parameter was tripled. Fig. 12 displays the *a*-*c* plot for Tables 5 and 6. The numbers near some symbols are the respectives EOP. As can be seen, the disordered samples (triangles) present higher c and lower a parameters, and low EOP. Nevertheless some ixiolite samples display EOP (e.g. 83%) similar to those calculated for columbite (e.g. 96%). Therefore, even some clearly disordered samples (ixiolite) can be misidentified with an ordered one (columbite).

The *a*-*c* plot shown in Fig. 13 summarizes the obtained results for synthetic samples (see Table 4). The ferrocolumbite and manganocolumbite samples follow the high EOP line (EOP≃96%-125%), as was observed for highly ordered natural samples. The $CuNb_2O_6$ samples, prepared at different laboratories, [17,39-41] but using similar routes, present anomalous EOP values (between -3% and -7%). Accordingly, in the *a*-*c* plot they follow the low EOP line. However, it is interesting to note that the sample $Cu_{0.36}Zn_{0.64}Nb_2O_6$ presents EOP=101%, typical of a highly ordered columbite. The available data do not enable us to elucidate this apparent contradiction. It is not possible to conclude if $CuNb_2O_6$ is a disordered sample, or if it is simply a quite distorted one, as previously suggested. It is interesting to point out that the c parameters for all $CuNb_2O_6$ samples are higher than 5.107 Åand that for $Cu_{0.36}Zn_{0.64}Nb_2O_6$ this parameter belongs to the range of the ordered samples, i.e. between 4.978 and 5.097 Å. The elongation of the c parameter is not correlated with the ionic radii of the concerned cations ($r_{Cu^{2+}} = 0.72$ Å; $r_{Zn^{2+}} = 0.82$ Å); it can be attributed to a strong Jahn-Teller effect.

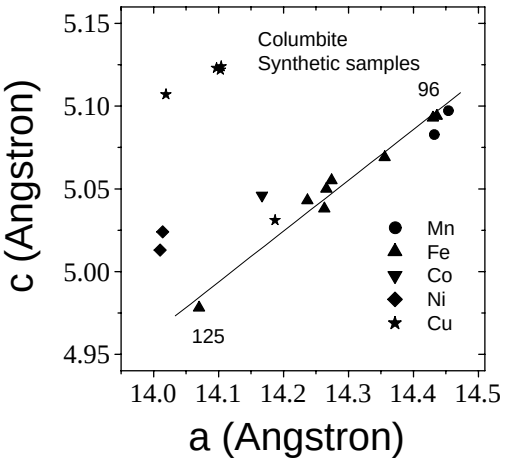

Figure 13. c-a plot for synthetic columbite samples. The number near the symbols are the respective EOP. Data from Table 4.

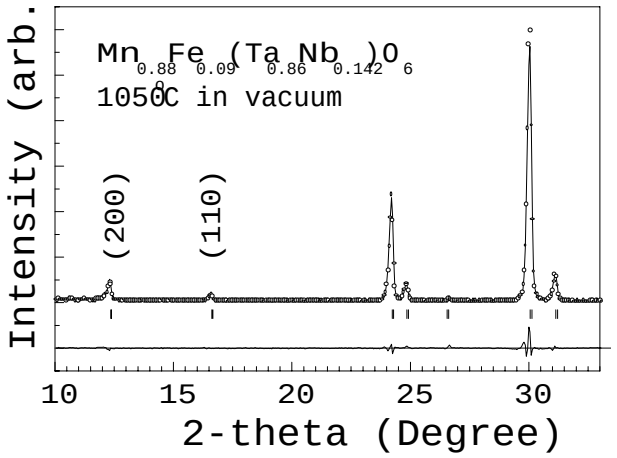

Figure 14. Representative part of the room-temperature X-ray powder diffraction pattern for the natural $Mn_{0.88}Fe_{0.09}Ta_{1.72}Nb_{0.28}O_6$ sample heated-treated in vacuum. Open circles, solid line and the lower trace as defined in Fig. 6.

Another way to evaluate cation order in tantalite-columbite species can be done by using MS, because it permits to easily differentiate between ixiolite and tantalite-columbite (or wodginite), as long as hyperfine interactions are very sensitive to change of the near-nearest environment. To the best of our knowledge Wenger *et al.*[11] were the first to report MS results concerning cation distribution in partially ordered columbite samples. Afterward we published[45, 52] MS studies of cation ordering on a natural manganocolumbite with composition $Mn_{0.88}Fe_{0.09}(Ta_{0.86}Nb_{0.14})_2O_6$, in the following named simply $MnFeTa_2O_6$. A similar study has been published for columbite-tantalite samples from San Luis pegmatite (Argentina). Other authors [45,52,55] have proposed the following parameter to quantify the cation order percentage

$$x(\%) = -50 + 1.515A_A, \qquad (2)$$

where A_A is the relative Mössbauer spectral area attributed to the A site of the AB_2O_6 structure.

Fig. 14 displays part of the XRD pattern for $MnFeTa_2O_6$ heated in vacuum at 1050 °C. This pattern is quite similar to that for the as-collected sample (Table 2), but shows a small increase in the relative intensity of the superstructure reflections. That is, I_{200}/I_{311}=0.08 and I_{110}/I_{311}=0.03, while for the as-collected sample, I_{200}/I_{311}=0.05 and I_{110}/I_{311}=0.02. Thus, it appears that it is not appropriate to use superstructure reflections to evaluate cation ordering in this case. The EOP, whose values for the as-collected and ordered sample are, respectively, 68% and 93%[45] appears to be more hopeful.

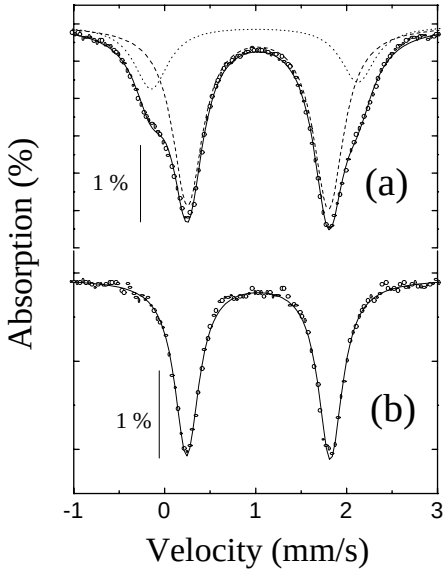

Figure 15. Mössbauer spectra taken at 300 K for: (a) as-collected natural sample; (b) powdered natural sample heat-treated in vacuum. Open circles represent observed data. Solid lines represent the calculated spectra based on a least-squares procedure. Smashed lines represent the calculated subspectra.

The MS spectra taken at room temperature for these samples are shown in Fig. 15. The spectrum for the as-collected sample, displayed in Fig. 15(a), was fitted to two doublets (see Table 7) with ^{57}Fe hyperfine parameters characteristic of Fe^{2+} high spin in octahedral coordination. One doublet should be attributed to Fe^{2+} in FeO_6 octahedra, while the other one should be attributed to Fe^{2+} in TaO_6 octahedra. Our results are quite similar to those reported by Wenger *et al.* [11,45,52,55] for a partially ordered columbite with composition

$(Fe_{0.65}Mn_{0.30}Ti_{0.05})(Nb_{0.75}Ta_{0.25})_2O_6$. Based on X-ray structure refinement these authors suggested that the FeO_6 octahedra are more distorted than the NbO_6 ones, and attributed the inner doublet to Fe^{2+} in the former octahedra, while the outer one was attributed to Fe^{2+} in NbO_6 octahedra. This same site assignment was adopted by Augsburger *et al.*[55] for similar samples.

As it is known, Δ is proportional to the electric field gradient (EFG) tensor, which has contributions from the external ligand charges (lattice contribution) and from the valence electrons (valence contribution). On the other hand, the valence contribution can be divided into two contributions: one from the crystal field (CF contribution) and other from the metal orbitals (MO contribution). For Fe^{2+} high spin the CF contribution dominates the valence contribution which is very temperature dependent. For several materials it can be demonstrated[56] that as the octahedral distortion increases, the quadrupole splitting decreases. On the contrary, for Fe^{3+} minerals the valence contribution is almost null and Δ is fully due to the lattice contribution. In this case Δ increases with the octahedral distortion and is less temperature dependent.

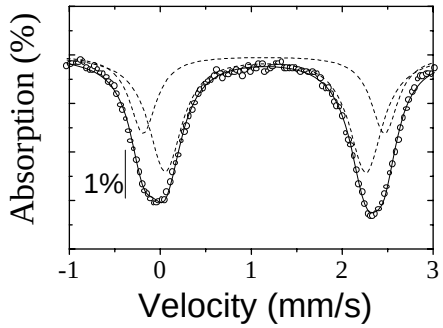

Figure 16. Mössbauer spectrum taken at 80 K for the as-collected natural sample. Open circles and smashed lines as defined in Fig. 15.

Nevertheless, site assignments following the above reasoning for Fe^{2+} high spin is not so straightforward. The above assignment is certainly correct, since the spectrum for the heated-in-vacuum sample was fitted to only one doublet with hyperfine parameters (see Table 7) almost the same as those used to fit the inner quadrupolar doublet. The disappearing of the outer quadrupolar doublet is a clear indication of cation ordering and enables us to attribute the inner doublet to Fe^{2+} in FeO_6 octahedra. However, to correlate octahedra distortion and Δ values, low temperature MS measurements should be performed. Sites with low distortions show Δ values more strongly dependent on temperature than those ones with high distortions. Figs. 15 and 16 and Table 7 show that from 300 K to 80 K the inner quadrupole splitting increases 42% (from 1.55 mm/s to 2.21 mm/s), while the outer one increases 18% (from 2.26 mm/s to 2.66 mm/s). Such a thermal evolution indicates that the outer doublet should be attributed to the more distorted octahedra, in clear contradiction with the previous findings.[11, 55]

IV Cation ordering versus oxidation of columbite

Heating experiments are, by far, the main source of data on the study of order-disorder phenomena in the ixiolite-columbite-wodginite system. To introduce the present discussion, it is interesting to highlight some statements found in the literature: 'When ixiolite is heated in air, several changes occur in the x-ray diffraction pattern.'[2] 'Disordered members of the columbite-tantalite group, (...), develop an ordered structure on heating at about 1000 °C (...).'[19] ' Pseudo-ixiolite, (...), is a complex Nb-Ta-oxide similar to ixiolite but with the difference that its structure may be inverted by heating (probably by ordering of the cations) to give an XRD pattern similar to columbite.'[49] 'Heating of samples in excess of 950 °C has been shown to induce cation order (...).'[54] Such descriptions of heating experiments are clearly incomplete. Some of them do not specify the atmosphere, and obviously heating in air, in a reducing atmosphere, or in vacuum will certainly produce different reactions. Also, heating a powdered or a crystal sample in air will produce different oxidation effects, because for the latter one the area available for oxidation is smaller. Therefore, these kind of experimental conditions need to be informed. Recently it was stated that heating coarse crystal fragments in air at 1000 °C for 16 h, induces cation order in columbite and results in no significant oxidation of bulk Fe^{2+}, as monitored by unit-cell parameters.[54] We have investigated these issues performing heating experiments on three different samples:[45, 52, 53] (i) crystal fragment of the natural manganocolumbite, $Mn_{0.88}Fe_{0.09}(Ta_{0.86}Nb_{0.14})_2O_6$; (ii) powdered specimen of the manganocolumbite; (iii) powder synthetic ferrocolumbite, $Fe(Ta_{0.4}Nb_{0.6})_2O_6$. Sample (i) was heated in air (the obtained sample was labeled NCH air). Part of the sample (ii) was used for the heating experiment in air (label PNH air), while the other part (label PNH vac) was pelleted and encapsulated in quartz ampoules under vacuum ($p \simeq 10^{-5}$ Pa). Sample (iii) was heated in air (label PSH air). All the samples were heated at 1320 K for 48 h and subsequently slowly cooled at 15 K/h. This cooling rate is adequate for cation ordering, e.g., all Fe+Mn in site A and all Ta+Nb in site B of the AB_2O_6 structure.[52]

Table 7: Hyperfine parameters for all measurements reported in the present work. As-coll, PNH vac, PNH air, NCH air, as-prep and PSH air stand for, respectively: untreated natural sample; powdered natural sample heat-treated in vacuum; natural sample heat-treated in air; crystal fragment of the natural sample heat-treated in air; as-prepared synthetic sample and powdered synthetic sample heat-treated in air. Δ is the quadrupole splitting at the iron sites; δ is the isomer shift relative to α-Fe; $\Gamma \pm 0.01$ is the linewidth at half-height; A is the site occupancy, given by the relative spectral area. Uncertainties on the last figures are reported in brackets.

Sample	Temp (K)	Δ (mm/s)	δ (mm/s)	Γ (mm/s)	A (%)	Site assignment
As-coll	300	1.55(5)	1.13(3)	0.40	71(4)	FeO_6
		2.26(7)	1.09(3)	0.47	29(1)	TaO_6
	80	2.21(7)	1.27(4)	0.44	66(3)	FeO_6
		2.66(8)	1.25(4)	0.35	34(2)	TaO_6
PNH vac.	300	1.58(5)	1.14(3)	0.32	100	FeO_6
	80	2.29(7)	1.27(4)	0.34	100	FeO_6
PNH air	300	0.52(2)	0.40(1)	0.31	78(4)	FeO_6
		0.34(1)	0.39(1)	0.33	22(1)	TaO_6
	80	0.59(2)	0.52(2)	0.30	52(3)	FeO_6
		0.40(1)	0.49(1)	0.28	48(2)	TaO_6
NCH air	300	0.55(2)	0.44(1)	0.44	29(1)	FeO_6
		0.32(1)	0.43(1)	0.41	25(1)	TaO_6
		1.51(4)	1.13(3)	0.47	41(2)	FeO_6
		2.26(7)	1.14(3)	0.43	5(2)	TaO_6
	80	0.61(2)	0.54(2)	0.33	28(1)	FeO_6
		0.43(1)	0.52(2)	0.30	24(1)	TaO_6
		2.17(6)	1.26(4)	0.38	26(1)	FeO_6
		2.59(8)	1.27(4)	0.37	22(1)	TaO_6
As-prep	300	1.78(5)	1.15(3)	0.32	100	FeO_6
	80	2.51(8)	1.27(4)	0.32	100	FeO_6
PSH air	300	0.37(1)	0.40(1)	0.30	100	FeO_6
	80	0.39(1)	0.51(2)	0.30	100	FeO_6

Representative parts of the XRD patterns for all the samples are shown in Fig. 17. A summary of the crystallographic parameters is displayed in Table 8. The PNH vac sample was discussed above. The XRD pattern for the PNH air sample was fitted to three phases. The major one was indexed to the space group C2/c, with lattice parameters (see Table 8) similar to those reported for wodginite from Rwanda.[4] Additional low intensity reflections can be attributed to monoclinic ixiolite with space group P2/c and lattice parameters quite close to those reported by Roth and Waring,[3] and to monoclinic $(Nb,Ta)_2O_5$ with space group P2 and lattice parameters similar to those reported in the JCPDS file 37-1468. The pattern attributed to wodginite ($MnFeTa_2O_8$) is well characterized by the existence of strong peaks at $d \simeq 2.95$Å$(2\theta \simeq 30.45°)$ and $d \simeq 2.98$ Å$(2\theta \simeq 29.98°)$ corresponding to (221) and $(\overline{2}21)$ reflections, respectively.

Therefore, heating the present powdered manganocolumbite sample in air, instead of order it, transforms it into a monoclinic compound quite similar to $MnFeTa_2O_8$, with minor reflections from a compound similar to ixiolite and the oxide $(Ta,Nb)_2O_5$. The present result confirms the data of Moreau and Tramasure.[5] These authors have synthesized a wodginite from the reaction Mn_2O_3+Ta_2O_5 at 1040 °C, for 95 h in air, suggesting that Mn plays an important role on the tantalite → wodginite transformation. We have also reproduced early results reported by Gouder de Beauregard et al.,[7] demonstrating that upon heating in air, $(Mn,Fe)Ta_2O_6$ shows a XRD pattern quite similar to that of $MnFeTa_2O_8$. Similar results have also been obtained by Turnock,[6] who showed that when synthesized in air, $MnFeTa_2O_8$ can be formed in a small composition range, just while there is sufficient Mn to fill the A site of the ABC_2O_8 structure, but does not form in the absence of Fe^{3+}. That is to say, part of the Fe atoms should pertains to the B site, while the Mn atoms and the other part of the Fe atoms can share the A site.

Table 8: Crystallographic parameters obtained in the present work. The sample labels are the same as defined in Table 7. Numbers in brackets designate $\pm 1\sigma$ on the last decimal given. R_B as defined in Table 2.

Sample	S.g.	a (Å)	b (Å)	c (Å)	$\beta(^\circ)$	R_B
PNH vac	Pbcn	14.3196(9)	5.7413(4)	5.0624(3)	90	5.76
PNH air	C2/c	8.779(4)	12.145(2)	5.089(1)	89.37	4.01
	P2/c	4.682(9)	5.647(28)	5.030(18)	90.14	2.13
	P2	20.429(2)	3.825(1)	19.461(3)	115.49	3.86
NCH air	Pbcn	14.3487(9)	5.7459(5)	5.0779(3)	90	1.22
	C2/c	9.0856(16)	12.0672(9)	5.0470(8)	88.29	2.34
	P2/c	4.7238(9)	5.6205(9)	5.0143(20)	90.81	1.24
	P2	20.4834(8)	3.8230(2)	19.4597(9)	115.38	1.57
As-prep	Pbcn	14.2737(2)	5.7354(1)	5.0554(1)	90	5.55
PSH air	P2/c	4.6493(8)	5.6221(7)	5.0089(7)	90.20	1.76
	P2	20.4022(27)	3.8322(3)	19.4007(16)	115.23	2.57

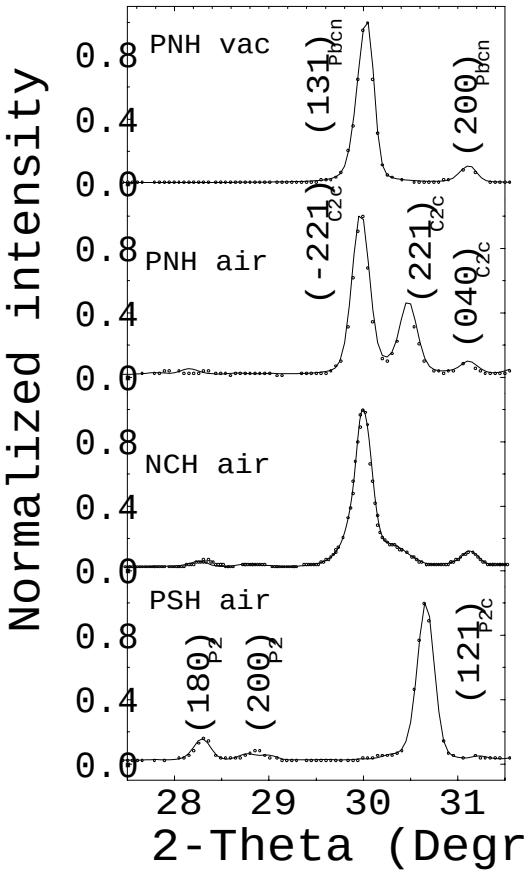

Figure 17. Representative parts of the X-ray powder diffraction patterns for all the heated-treated samples: powdered natural heated in vacuum (PNH vac), powdered natural heated in air (PNH air), fragments of natural crystal heated in air (NCH air) and powdered synthetic heated in air (PSH air). Open circles and solid lines as defined in Figure 6. Tantalite, wodginite, ixiolite and $(Nb,Ta)_2O_5$ reflections are indicated, respectively, by Pbcn, C2c, P2c and P2.

It is interesting to point out that although the results from Gouder de Beauregard *et al.*[7] are more than 30 years old, there is, to our knowledge, only the Graham and Thornber[8] effort to re-examine the $(Mn,Fe)Ta_2O_6 \rightarrow MnFeTa_2O_8$ transformation. Yet recent papers[11, 19, 25, 48, 51, 54] have casually dismissed this subject, although they have discussed the related subject $(Mn,Fe,Ta)O_2 \rightarrow MnFeTa_2O_8$ transition.

Differently, for the NCH air the reflections attributed to $MnFeTa_2O_8$ are clearly less intense as compared to those observed for PNH air (Fig. 17). Note, for instance, the strong decrease of (221) reflection. Following the refinement procedure it can be seen that the effect of heating a crystal sample is to produce a mixture of four phases; that one in large amount (label Pbcn) is the ordered $(Mn,Fe)Ta_2O_6$. Minor reflections were indexed to $MnFeTa_2O_8$, $(Mn,Fe)(Ta,Nb)O_4$ and $(Ta,Nb)_2O_5$. The former arrives from cation ordering in the bulk portion of the sample, while the minor contribution result from the near-surface oxidation.

The synthetic $Fe(Nb,Ta)_2O_6$ was used as a first check for the role played by Mn. The XRD pattern for PSH air was indexed to a mixture of two phases. The major one is monoclinic ixiolite, with space group P2/c and lattice parameters similar to those reported above for the PNH air sample. The phase with weak reflections (label P2) is the monoclinic oxide $(Nb,Ta)_2O_5$, also reported above for PNH air sample. Therefore, supposing cation conservation during the oxidation process and taking into account the XRD results, the compound $Fe(Nb_{0.6}Ta_{0.4})O_4$, hereafter $Fe(Nb,Ta)O_4$, with structure similar to ixiolite is the main product resulting from the oxidation of the synthetic ferrocolumbite $Fe(Nb,Ta)_2O_6$.

To improve our interpretation we have performed MS measurements of the samples analyzed by XRD. Fig. 18 shows the spectra taken at 300 K for PNH air and NCH air samples. First of all, there is no Fe^{2+}

contribution for the PNH air spectrum, which was fitted to two doublets with Δ = 0.52 mm/s and Δ = 0.34 mm/s (see Table 7), attributed to high spin Fe^{3+} in octahedral coordination. As discussed above, there are two different sites for Fe^{3+} in the wodginite structure: one of them is the B site and the other is the C site. Bearing in mind the great similarity between the outer doublet and that reported (Δ = 0.54 mm/s, δ=0.39 mm/s) for a synthetic Fe^{3+}-rich wodginite,[51] we have attributed the larger quadrupole splitting to Fe^{3+} at FeO_6 octahedra (site B) and the smallest one to Fe^{3+} at TaO_6 octahedra (site C). As discussed below, the smallest quadrupole is also quite similar to that attributed to ixiolite-like $Fe(Nb,Ta)O_4$, so that it is reasonable to suppose a mixture of contributions from wodginite site C and $Fe(Nb,Ta)O_4$. This is consistent with the XRD result, suggesting the tantalite $\rightarrow$ wodginite transformation, i.e., $(Fe^{2+},Mn)(Ta,Nb)_2O_6 \rightarrow MnFe^{3+}(Ta,Nb)_2O_8$.

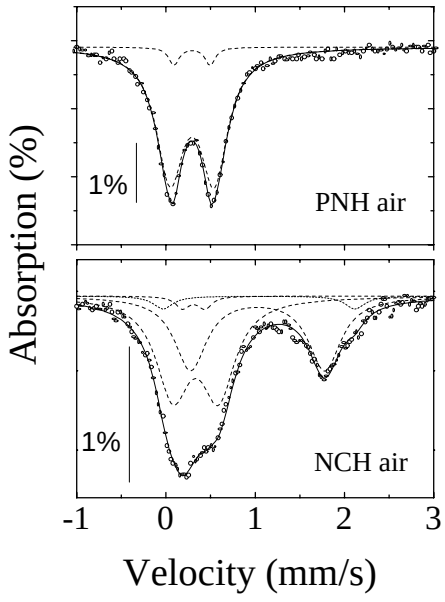

Figure 18. Mössbauer spectra taken at 300 K for PNH air and NCH air (labels defined in Fig. 17). Open circles and smashed lines as defined in Fig. 15.

The XRD results have shown that the effect of heating in air a crystal fragment of the $(Mn,Fe)Ta_2O_6$ sample is to produce a mixture of ordered $(Mn,Fe)Ta_2O_6$ and $MnFeTa_2O_8$, with minor reflections indexed to $(Fe,Mn)(Ta,Nb)O_4$ and $(Nb,Ta)_2O_5$. Consequently complex Mössbauer spectra are expected for this kind of sample. In fact, as shown in Fig. 18, the RT spectrum for the NCH air sample clearly contains contribution from Fe^{2+} and Fe^{3+} ions. This spectrum was fitted to four doublets: Δ=0.55 mm/s, Δ =0.32 mm/s, Δ =1.51 mm/s and Δ =2.26 mm/s. The site assignment followed that used before for the as-collected and PNH air samples. Thus, Δ=0.55 mm/s and Δ=1.51 mm/s are attributed, respectively, to Fe^{3+} and Fe^{2+} at FeO_6 octahedra, while Δ=0.32 mm/s and Δ=2.26 mm/s are attributed, respectively, to Fe^{3+} and Fe^{2+} at TaO_6 octahedra.

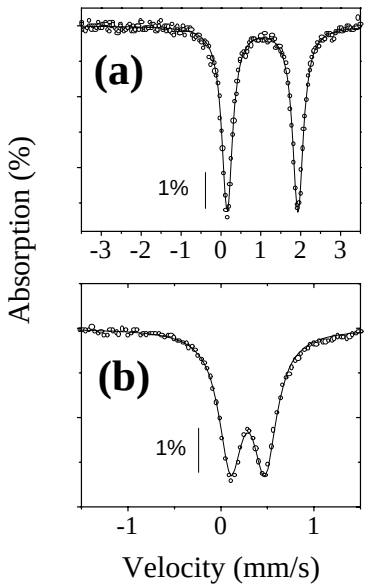

Figure 19. Mössbauer spectra taken at 300 K for: (a) as-prepared $Fe(Ta_{0.4}Nb_{0.6})_2O_6$ sample; (b) synthetic sample heated in air. Open circles and smashed lines as defined in Fig. 15.

To validate some of the hyperfine parameters used to fit the natural samples, we have submitted the synthetic $Fe(Nb_{0.6}Ta_{0.4})_2O_6$ sample to similar studies. The Mössbauer spectrum at room temperature for the as-prepared sample is shown in Fig. 19(a). The existence of only one narrow doublet is indicative of high degree cation ordering. It was fitted (see Table 7) to Δ=1.78 mm/s and δ=1.15 mm/s. These hyperfine parameters are close to those early reported for $FeNb_2O_6$.[16, 57] We have also measured this sample at 85 K.[45, 53] The relative increasing of the quadrupole splitting from 300 to 85 K is remarkably similar to that reported for $FeNb_2O_6$.[16] The spectrum measured at 300 K for the synthetic sample heated in air, displayed in Fig. 19(b), was fitted to a doublet attributed to Fe^{3+}, with Δ=0.37 mm/s and δ=0.40 mm/s. From the X-ray measurements this sample was identified as

$Fe(Nb,Ta)O_4$. Schmidbauer and Schneider reported similar results for a synthetic $FeNbO_4$ sample.[58]

Now, it is interesting to evaluate the consistence of our Mössbauer measurements. For the Mn-rich natural sample $(Mn,Fe)Ta_2O_6$ submitted to cation ordering we have observed just one quadrupole doublet, with Δ=1.58 mm/s. This quadrupole splitting is smaller than that reported for $FeNb_2O_6$ (Δ=1.70 mm/s).[16] These distinct values for Δ should be due to distinct Mn/Fe and Ta/Nb ratio concentrations. This hypothesis can be analyzed by considering the results from the synthetic $Fe(Nb_{0.6}Ta_{0.4})_2O_6$, for which we have measured Δ=1.78 mm/s. By comparing these hyperfine parameters it is reasonable to ascribe a small effect to the homopolar substitution Ta $\leftrightarrow$ Nb. The situation is quite different when $FeNb_2O_6$ and $(Mn,Fe)Ta_2O_6$ are compared. In this case the measurements indicate that the homopolar substitution Mn$\leftrightarrow$Fe is more effective in changing the hyperfine parameters (1.70 mm/s versus 1.58 mm/s) than the Ta$\leftrightarrow$Nb one (1.70 mm/s versus 1.78 mm/s). Considering the interdependence between quadrupole splitting and distortions of the metal-oxygen octahedra, and taking into account the ionic radii, these results seem to be consistent, since $(R_{Mn^{2+}}/R_{Fe^{2+}}) \simeq 1.08$, while $(R_{Nb^{5+}}/R_{Ta^{5+}}) \simeq 1.01$. Therefore, confirming previous structure refinement in similar samples[11] the effect of the homopolar substitution Mn$\leftrightarrow$Fe on the distortions of the metal-oxygen ocathedra (MO_6) is strongest than that produced by the Ta$\leftrightarrow$Nb one.

Concerning the PSH air sample a similar scenery can be obtained. For this sample we have obtained Δ=0.37 mm/s, a doublet attributed to the orthorhombic compound $Fe(Nb,Ta)O_4$. For the tetragonal compound $FeTaO_4$, with the rutile structure, it was reported Δ=0.53 mm/s.[59] As the homopolar substitution Ta$\leftrightarrow$Nb presents a minor effect on the hyperfine parameters of these compounds (see the results for $FeNbO_4$[58]), the reported results strongly suggest that the hyperfine parameters are more dependent on the crystal structure. Thus, if for columbite (orthorhombic $FeNb_2O_6$) $\Delta \simeq 1.70$ mm/s, and for tapiolite (tetragonal $FeTa_2O_6$) $\Delta \simeq 3.0$ mm/s[10, 28], it appears reasonable that Δ for ixiolite-like $Fe(Nb,Ta)O_4$ should be smaller than for rutile $FeTaO_4$. This becomes consistent if we take into account the interrelation between crystal structures. That is to say, the substructures (ixiolite and rutile) preserve the interrelation observed between the superstructures (columbite and tapiolite).

V Concluding remarks

The orthorhombic $(Fe,Mn)(Ta,Nb)_2O_6$ series presents continuous solid solutions on the $FeNb_2O_6$ - $MnNb_2O_6$ and on the $MnNb_2O_6$ - $MnTa_2O_6$ boundaries, but has solubility limit for $FeTa_2O_6$ less than 50%. In any case the Vegard's law is obeyed, mainly for synthetic samples. Order-disorder phenomena have been extensively investigated in this system, and an illustrative systematic have been obtained in terms of the *c*- and *a*-cell parameters. The more disordered samples are those with the higher *c/a* ratios. Contrary, the more ordered ones are those with the smallest *c/a* ratios.

Heating in air a partially ordered tantalite yields different results depending on the form of the sample. For a powder sample, the tantalite $\rightarrow$ wodginite transformation has been observed, in addition to minor contribution from ixiolite-like $FeTaO_4$ and Ta_2O_5. For a crystal fragment, the heat treatment in air produced a mixture of four phases: that one in large amount is the ordered tantalite, while minor contributions are attributed to wodginite, $FeTaO_4$ and Ta_2O_5. The former arrives from cation ordering in the bulk portion of the sample, while the minor contributions result from the near-surface oxidation. The Mn content as well as the oxidant atmosphere appears to play an important role on the tantalite $\rightarrow$ wodginite transformation. The same heat treatment applied to a powder synthetic ferrocolumbite induces a different reaction: the sample is transformed into $FeNbO_4$ with minor amount of Nb_2O_5.

Acknowledgments

We would like to thank Dr. M. Adusumilli (UNB, Brazil) and Company for Research of Mineral Resources (CPRM) for providing us with the natural samples; to Dr. J.-Y. Henri (DRFMC/CENG, Grenoble) for providing us with the synthetic ferrocolumbite; to Dr. M.A.Z. Vasconcellos for the EPMA analyses. Valuable discussions with Prof. F. C. Zawislak are gratefully acknowledged. This work was supported in part by the Brazilian agencies CAPES, CNPq, FAPERGS and FINEP.

References

[1] E.H. Nickel, J.F. Rowland and R.C. McAdam, Can. Mineral. **7**, 390 (1963).

[2] E.H. Nickel, J.F. Rowland and R.C. McAdam, Am. Mineral. **48**, 961 (1963).

[3] R.S. Roth and J.L. Waring, Am. Mineral. **49**, 242 (1964).

[4] P. Bourguignon and J. Mlon, Ann. Soc. Gol. Belgique **88**, 291 (1965).

[5] J. Moreau and G. Tramasure, Ann. Soc. Gol. Belgique **88**, 301 (1965).

[6] A.C. Turnock, Can. Mineral. **8**, 461 (1966).

[7] C. G. Gouder de Beauregard, J. Dubois and P. Bourguignon, Ann. Soc. Gol. Belgique **90**, 501 (1967).

[8] J. Graham and M.R. Thornber, Am. Mineral. **29**, 1026 (1974).

[9] M.S. Adusumilli, Contribution to the Mineralogy of Niobotantalites from the Northeast Province, PhD Thesis, Universidade Federal de Minas Gerais, Brazil. (in Portuguese), 1976.

[10] S.M. Eicher, J.E. Greedan and K.J. Lushington J. Sol. State Chem. **62**, 220 (1986).

[11] M. Wenger, T. Armbruster and C.A. Geiger, Am. Mineral. **76**, 1897 (1991).

[12] C.A. dos Santos and J. Oliveira, Solid State Commun. **82**, 89 (1992).

[13] R.K. Kremer and J.E. Greedan, J. Sol. State Chem. **73**, 579 (1988).

[14] V.D. Mello, L.I. Zawislak, J.B. Marimon da Cunha, E.J. Kinast, J.B. Soares, C.A. dos Santos, J. Magn. Magn. Mater. **196-197**, 846 (1999).

[15] V. Antonietti, E.J. Kinast, L.I. Zawislak, J.B.M. da Cunha and C.A. dos Santos, J. Phys. Chem. Solids **62**, 1239 (2001).

[16] M. Eibschtz, U. Ganiel and S. Shtrikman, Phys. Rev. **156**, 259 (1967).

[17] M.G.B. Drew, R.J. Hobson and V.T. Padayatchy, J. Mater. Chem. **3**, 889 (1993).

[18] C. Heid, H. Weitzel, F. Bourdarot, R. Calenczuk, T. Vogt and H. Fuess, J. Phys.:Condens. Matter **8**, 10609 (1996).

[19] P. Cerny and T.S. Ercit, Bull. Minral. **108**, 499 (1985).

[20] R.W. Hutchison. Am. Mineral. **40**, 432 (1955).

[21] C. Hutton. Am. Mineral. **44**, 9 (1959).

[22] J.D. Grice, R.B. Ferguson and F.C. Hawthorne, Can. Mineral. **14**, 540 (1976).

[23] R.B. Ferguson, F.C. Hawthorne and J.D. Grice, Can. Mineral. **14**, 550 (1976).

[24] A.M. Clark, E.E. Fejer. Mineral. Mag. **42**, 477 (1978).

[25] T.S. Ercit, F.C. Hawthorne and P. Cerny, Can. Mineral. **30**, 597 (1992).

[26] M.A. Wise and P. Cerny, Can. Mineral. **34**, 631 (1996).

[27] A. Aruga, E. Tokizakik, I. Nakai and Y Sugitami, Acta Crystallogr. C **41**, 663 (1985).

[28] L.I. Zawislak, J.B.M. da Cunha, A. Vasquez and C.A. dos Santos, Solid State Commun. **94**, 345 (1995).

[29] L.I. Zawislak, G.L.F. Fraga, J.B. Marimon da Cunha, D. Schmitt, A.S. Carriço, C.A. dos Santos, J. Phys.: Condens. Matter **9**, 2295 (1997).

[30] J.N. Reimers, J.E. Greedan, C.V. Stager, R. Kremer, J. Solid State Chem. **83**, 20 (1989).

[31] M.E. Fisher, D.R. Nelson, Phys. Rev. Lett. **32**, 1350 (1974).

[32] A. Aharony, Phys. Rev. Lett. **34**, 590 (1975).

[33] A. Aharony, S. Fishman, Phys. Rev. Lett. **37**, 1587 (1976).

[34] H. Kadowaki, H. Yoshizawa, M. Itoh, I. Yamada, J. Phys. Soc. Jpn. **59**, 713 (1990).

[35] W.A.H.M. Vlak, E. Frikkee, A.F.M. Arts, H.W. de Wijn, J. Phys. C: Solid State Phys. **16**, L1015 (1983).

[36] I. Yaeger, A.H. Morrish and B.M. Wanklyn, Phys. Rev. B **15**, 1465 (1977).

[37] H. Weitzel. Z. Kristallogr. **144**, 238 (1976).

[38] T. Hanawa, M. Ishikawa and K. Miyatani. J. Phys. Soc. Japan **61**, 4287 (1992).

[39] B. Kratzheller and R. Gruehn, J. Alloys and Compounds **183**, 75 (1992).

[40] M. Sato and Y Hama, J. Solid State Chem. **118**, 193 (1995).

[41] J. Norwig, H. Weitzel, H. Paulus, G. Lautenschlger, J. Rodriguez-Carvajal and H. Fuess, J. Solid State Chem. **115**, 476 (1995).

[42] P. Cerny, W.L. Roberts, T.S. Ercit and R. Chapman, Am. Mineral. **70**, 1044 (1985).

[43] M.N. Spilde and C.K. Shearer, Can. Mineral. **30**, 719 (1992).

[44] T. Mulja, A.E. Williams-Jones, R.F. Martin and S.A. Wood, Am. Mineral. **81**, 146 (1996).

[45] C.A. dos Santos, L.I. Zawislak, V. Antonietti, E.J. Kinast and J.B.M. da Cunha, J. Phys.: Condens. Matter **11**, 7021 (1999).

[46] E.J. Kinast. *Structural refinement with the Rietveld method: implementation and essays with the program Fullprof.* MSc dissertation (in Portuguese). Instituto de Física - UFRGS, 2000.

[47] M.A. Wise, A.C. Turnock and P. Cerny, Neues Jahrb. Mineral. H **8**, 372 (1985).

[48] P. Cerny, T.S. Ercit and M.A. Wise, Can. Mineral. **30**, 587 (1992).

[49] P. Cerny and A.C. Turnock, Can. Mineral. **10**, 755 (1971).

[50] P. Cerny, T.S. Ercit, M.A. Wise, R. Chapman and H.M. Buck, Can. Mineral. **36**, 547 (1998).

[51] T.S. Ercit, P. Cerny, F.C. Hawthorne and C.A. McCammon, Can. Mineral. **30**, 613 (1992).

[52] L.I. Zawislak, V. Antonietti, J.B.M. da Cunha and C.A. dos Santos Solid State Commun. **101**, 767 (1997).

[53] V. Antonietti, *Order-disorder transformations on the ixiolite-columbite-wodginite system.* MSc dissertation (in Portuguese). Instituto de Física - UFRGS, 2000.

[54] T.S. Ercit, M.A.R. Wise and P. Cerny. Am. Mineral. **80**, 613 (1995).

[55] M.S. Augsburger, J.C. Pedregosa, G.M. Sosa and R.C. Mercader. J. Solid State Chem. **143**, 219 (1999).

[56] G.M. Bancroft, *Mössbauer Spectroscopy. An Introduction for Inorganic Chemists and Geochemists*, McGraw-Hill, London (1973).

[57] I. Yaeger, A.H. Morrish, C. Boumford, C.P. Wong, B.M. Wanklyn and B.J. Garrard. Solid State Comm. **28**, 651 (1978).

[58] E. Schmidbauer and J. Schneider. J. Sol. State Chem. **134**, 253 (1997).

[59] D.N. Astrov, N.A. Kryukova, R.B. Zorin, V.A. Makarov, R.P. Ozerov, F.A. Rozhdestrvenskii, V.P. Smirnov, A.M. Turchaninov and N.V. Fadeeva. Sov. Phys. - Cryst. **17**, 1017 (1973).